J. exp. Biol. 150, 321–342 (1990)
Printed in Great Britain © The Company of Biologists Limited 1990

FAST-START PERFORMANCE OF RAINBOW TROUT *SALMO GAIRDNERI* AND NORTHERN PIKE *ESOX LUCIUS*

BY DAVID G. HARPER AND ROBERT W. BLAKE
Department of Zoology, University of British Columbia, Vancouver, V6T 2A9 Canada

Accepted 9 January 1990

Summary

The escape performances of rainbow trout *Salmo gairdneri* (Richardson) and northern pike *Esox lucius* (Linnaeus) (mean lengths 0.32 m and 0.38 m, respectively) were measured with subcutaneously implanted accelerometers. Acceleration–time plots reveal two types of fast-starts for trout and three for pike. Simultaneous high-speed ciné films demonstrate a kinematic basis for these differences. Trout performing C-shaped fast-starts produce a unimodal acceleration–time plot (type I) while during S-shaped fast-starts a bimodal acceleration–time plot (type II) results. Pike also exhibit similar type I and II fast-starts, but also execute a second S-shaped fast-start that does not involve a net change of direction. This is characterized by a trimodal acceleration–time plot (type III).

Intraspecific and interspecific comparisons of distance, time, mean and maximum velocity, and mean and maximum acceleration rate indicate that fast-start performance is significantly higher for pike than for trout, for all performance parameters. This indicates that performance is related to body form. Overall mean maximum acceleration rates for pike were $120.2\pm20.0\,m\,s^{-2}$ and $59.7\pm8.3\,m\,s^{-2}$ for trout.

Performance values directly measured from the accelerometers exceed those previously reported. Maximum acceleration rates for single events reach $97.8\,m\,s^{-2}$ and $244.9\,m\,s^{-2}$ for trout and pike, respectively. Maximum final velocities of $7.06\,m\,s^{-2}$ ($18.95\,L\,s^{-1}$) were observed for pike and $4.19\,m\,s^{-2}$ ($13.09\,L\,s^{-1}$) for trout, where L is body length; overall mean maximum velocities were $2.77\,m\,s^{-2}$ for trout and $3.97\,m\,s^{-2}$ for pike.

Introduction

Fast-starts (sudden, high-energy bursts of unsteady swimming activity) are of great biological importance because they are employed by most fish when escaping life-threatening situations, and by some fish as a means of attaining prey. Fish that do not execute fast-starts depend on other mechanisms (armour, spines, poisons, camouflage, etc.) to ward off potential predators.

Early studies on fish fast-starts (Gero, 1952; Gray, 1953; Hertel, 1966; Fierstine and Walters, 1968; Weihs, 1973) qualitatively investigated kinematics and reported

Key words: fast-starts, *Salmo*, *Esox*, acceleration, accelerometry.

maximum acceleration rates of 40–50 $m\,s^{-2}$. Webb (1975) suggested that, to evaluate fast-start performance properly, data for the duration of the event, mean and maximum accelerations, mean and maximum velocities and the distance covered must all be reported. Since then, several studies (Eaton *et al.* 1977, 1988; Webb, 1978*a*,*b*; Webb and Skadsen, 1980) have suggested that displacement alone is adequate to evaluate fast-start performance. However, some models estimating thrust and energetics during fast-starts incorporate performance variables other than displacement (e.g. Weihs, 1973; Lighthill, 1975; Harper and Blake, 1988).

High-speed (200–250 Hz) cinematography has been employed to evaluate more specific aspects of fast-starts, such as predator and prey latency periods (Webb, 1984; Eaton *et al.* 1977, respectively) and the effects of size, median-fin amputation, temperature and body form on escape performance (Webb, 1976, 1977, 1978*a*,*b*, respectively). Rand and Lauder (1981), employing the same methodology, correlated feeding and locomotor behaviour, while Webb and Corolla (1981) investigated the burst swimming performance of larvae.

Few investigations have employed methodologies other than film analysis to study fast-start performance. DuBois *et al.* (1976) inserted a biaxial accelerometer into the stomach of a bluefish, *Pomatomus saltatrix*, and measured escape accelerations. Unfortunately they did not consider the location of their accelerometer relative to the combined centre of mass of the fish and accelerometer. In addition, the fish was 'scared' shortly (5–20 min) after previous bouts of steady and unsteady activity, so probably performing sub-maximally.

Other studies include an investigation of caudal fin strains during fast-starts using rosette strain gauges (Lauder, 1982) and studies on the reticulospinal command mechanisms involved in escape behaviour in fish (Eaton *et al.* 1984, 1988). None of these evaluated swimming performance.

Here, the escape performances of trout and pike are determined by accelerometry and cinematography. Two species of fish, with different body forms, are observed to test the hypothesis that mean and maximum accelerations during fast-starts are independent of body form (Webb, 1978*b*).

Materials and methods

Two species of fish were used in this study, northern pike *Esox lucius* (N=4, mass=0.396±0.058 kg, fork-length=0.378±0.019 m: mean±2 S.E.) and rainbow trout *Salmo gairdneri* (N=8, mass=0.318±0.063 kg, fork-length=0.316±0.020 m: mean±2 S.E.). The pike were seined from Baptiste Lake in northern Alberta; trout were obtained from a local (British Columbia) fish hatchery. Healthy adults were held for 6–12 months in 1000-l circular outdoor holding tanks (2 m in diameter) which were flushed continuously with fresh water at 15–20 °C. Fast-start performance is independent of temperature over this range (Webb, 1978*a*). Trout were fed trout chow daily, and pike were fed live goldfish thrice weekly until ready for use.

The experimental arena, made of glass and Plexiglas, measured 2.45 m

1.22 m×0.47 m and was filled to a depth of approximately 0.30 m. A 0.02 m grid was placed on the bottom of the arena and fresh water, from the same supply as that of the outdoor holding tanks, was slowly circulated, except during filming. Fish were allowed 48 h to acclimate to the aquarium before experimentation and were not fed during that time.

Measurement of acceleration

Accelerations were directly measured with a Kistler 8616-A1000 low-impedance piezoelectric accelerometer (range±1000 *g*; frequency response 125 kHz; cylindrical dimensions 0.0058 m×0.0051 m diameter; mass<0.0005 kg). Acceleration–time data were stored in the mainframe memory of a Nicolet 4094 digital oscilloscope, transferred to floppy disk, and later to an Olivetti M24 PC.

Fish were quickly anaesthetized in 0.0002 kg l^{-1} MS222 buffered with 0.0004 kg l^{-1} sodium bicarbonate. Once anaesthetized, fish were transferred to a 'wet' table where a recirculating pump continuously flushed one-third strength anaesthetic over the gills. For a description of the anaesthetizing procedure, see Richardson (1985).

The accelerometer was easily implanted subcutaneously. The incision was made above the centre of mass, parallel to the centre-line of the fish, just lateral to the vertebral column. Centre of mass was assumed to be 0.41×fork-length (measured from the nose to the middle of the caudal fin trailing edge) for pike and at the leading edge of the dorsal fin for trout (Webb, 1978*b*). The small mass of the accelerometer (<0.2 % of fish mass for the smallest specimen) eliminated the need to reconsider the location of the centre of mass after implantation. The incision was never longer or deeper than about 1 cm, involved no tissue removal, and no significant loss of blood. Once the accelerometer was implanted, the incision was tightly closed using Ethicon V-5 tapercut cardiovascular sutures. The shape of the incision and the tight closure prevented the accelerometer from altering its orientation in the fish during experiments.

Fish were then placed in a recovery tank where fresh water was flushed over the gills until normal opercular activity resumed. At this point the fish was re-introduced to the experimental arena and allowed to recover for 24 h. No deaths could be attributed to the incision or anaesthetization.

When a fish was still, in the centre of the tank, it was startled by thrusting a wooden pole towards its head, perpendicular to its longitudinal axis. This produced a high-performance escape behaviour because the startle response is an all-or-none maximum response (Eaton *et al.* 1977). The tank was of sufficient size for the walls not to interfere with the escapes. A method for startling fish by electric shock (Webb, 1975) was employed in preliminary experiments but elicited less forceful fast-starts. A recovery period of several hours was allowed between test runs.

Accelerometer calibration

The accelerometer was calibrated on a 'guillotine-like' apparatus which pro-

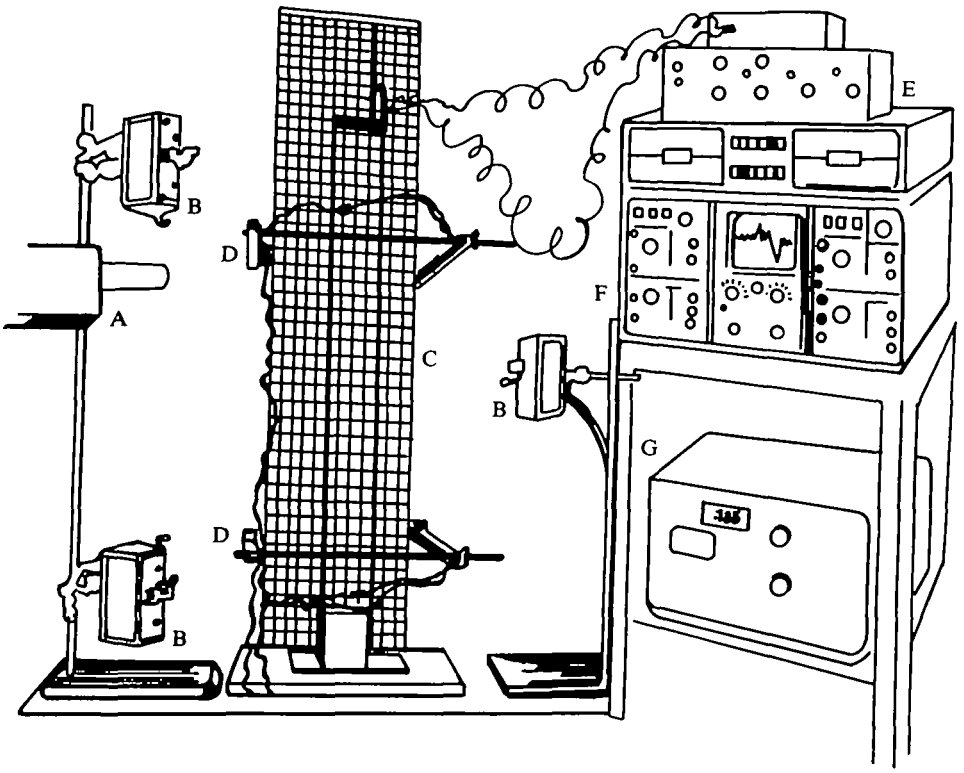

Fig. 1. Schematic diagram of the accelerometer calibration apparatus. The time of the drop is measured as the bar travels from the upper to the lower set of infrared timing lights (D). Other equipment includes the camera (A), lights (B), free-fall apparatus (C), accelerometer power source and amplifier (E), oscilloscope (F) and digital clock (G).

vided constant 'free-fall' acceleration. The apparatus (Fig. 1) consists of a brass bar (mass=1 kg) which slides down parallel steel rods. Two sets of infrared lights and sensors were positioned 0.50 m apart near the top and bottom of the rods. These input to a digital clock which measured the time of the drop; the first set of sensors starting, and the second set stopping the clock. The elapsed time was used to determine the actual acceleration of the bar by employing the standard relationship for free-falling objects:

$$a=2\Delta d t^{-2} \tag{1}$$

(Tilley and Thumm, 1974), where a is acceleration, d is distance and t is time. The time measured was that of the latter portion of the drop, corresponding to the position of the infrared sensors. These were set further down the rods so that interference with the start lever (which sets the bar into motion) could be neglected.

The total distance of the drop (Δd_T) is 0.68 m, of which the last 0.50 m (Δd_2) is

timed; the initial 0.18 m (Δd_1) is not. The measured time (t_2) is the difference between total drop time (t_T) and the time to fall to the first set of sensors (t_1):

$$t_2 = t_T - t_1 , \tag{2}$$

which was measured as 0.185±0.001 s (N=40; mean±2 S.E.). Rearranging equation 1 and substituting values for Δd_T and Δd_1 gives:

$$t_T = \left(\frac{2\times 0.68}{a}\right)^{1/2} \tag{3}$$

and

$$t_1 = \left(\frac{2\times 0.18}{a}\right)^{1/2} . \tag{4}$$

Substituting equations 3 and 4 and the measured value for t_2 into equation 2 gives:

$$0.185 = \left(\frac{1.36}{a}\right)^{1/2} - \left(\frac{0.36}{a}\right)^{1/2} . \tag{5}$$

Solving for a gives a value of 9.37 m s^{-2}. The difference between this value and the standard gravitational constant (g=9.81 m s^{-2}) can be attributed to the friction on the rods and air resistance.

The accelerometer was affixed to the brass bar with modelling clay, in the same orientation as in the fish. Accelerations from 40 further drops were then recorded on the oscilloscope. Fig. 2 is an example of one such calibration. The raw accelerometer data are smoothed because vibrations in the apparatus created high-frequency noise. This noise also accounts for the data points located below zero before the bar is dropped. The resulting curve (Fig. 2) indicates low-frequency variations, which are due to instability (vibration) in the apparatus. In the still fish, flat-line signals were recorded from the accelerometers.

The average signal strength was 148±6 mV (mean±2 S.E.), which translates to 155 mV g^{-1}, after accounting for frictional resistance. Subsequent trials, involving changes of orientation of the accelerometer, confirmed that it is equally sensitive in the reverse direction and insensitive when oriented sideways (parallel with the ground).

Cinematography

Accelerating fish were filmed with a 16 mm high-speed ciné camera (Locam model 51-0002) on Kodak 7250 400 ISO ciné film at 50–350 Hz. Fish were filmed as if from above by mounting a 2.45 m×1.22 m mirror at 45° over the tank. When filming pike, illumination was provided by two Berkey Beam 800 spot/flood lights mounted in front of the arena and shone into the mirror. For trout, four Crown 650 video lights were directed through the sides of the arena, below water level.

Processed films were analyzed on an image analyzer (Photographic Analysis Limited Projection Analysis Unit, ZAE 76). The system includes a variable-speed projector, a ground-glass viewing/digitizing tablet and a digitizing computer.

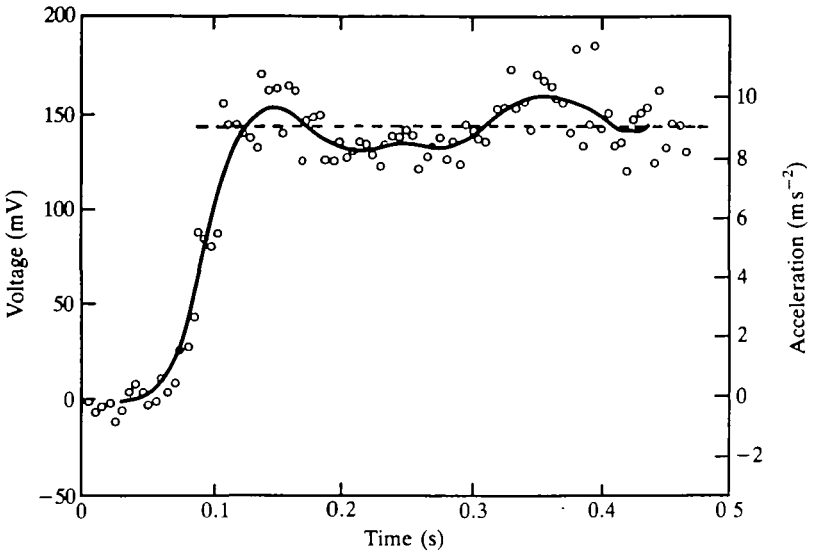

Fig. 2. Example of an accelerometer calibration trace. Voltage is indicated on the left axis and the corresponding acceleration on the right. Open circles represent every 100th accelerometer data point. The solid line is the smoothed accelerometer data. The dashed line is the average acceleration of the timed portion.

Images of the accelerating fish were directed onto the tablet and frame-by-frame tracings of the fish were made.

Calculation of velocity and distance

The derivation of velocity from acceleration data involves an integration with respect to time. Distance can then be obtained by a second integration, performed on the resultant velocity–time data. In the following procedure it is assumed that the acceleration between data points is such that the curve can be considered as a series of straight lines connecting these points. The small time interval (0.00001 s) between data points supports this assumption.

Since, by definition, fast-starts originate from an idle position, the velocity and acceleration at time T_0 are also zero (V_0=0; a_0=0). The velocity (V_i) at time T_i is approximated by numerical integration using the following formula:

$$V_i = V_0 + \sum_{i=1}^{n} \frac{(a_{i-1} + a_i)}{2} \Delta t . \tag{6}$$

The distance moved can be derived from the velocity data in the same way:

$$D_i = D_0 + \sum_{i=1}^{n} \frac{(V_{i-1} + V_i)}{2} \Delta t . \tag{7}$$

Correction for rotational acceleration

The curvilinear nature of the escape trajectories introduces accelerations that are detected by the accelerometer. This results from the fact that bodies accelerating along a curved trajectory realize, along with the centripetal acceleration directed towards the centre of rotation, a component parallel to the tangent of the trajectory (Meriam, 1975). This will be referred to as tangential acceleration, an artefact resulting from non-linear motion which must be subtracted from the accelerometer values.

Film data were used to determine the tangential acceleration, which is equal to the product of the angular acceleration and the radius of the curve. To determine these values, the position of the accelerometer (easy to locate from the incision scar), at each time point, was plotted, giving the trajectory traced out during the escape. The centre of rotation was determined by locating the intercept of perpendicular lines drawn from tangents to the curve. The distance from the curve to the intercept is the radius.

The angular acceleration is given by the rate of change of the angular velocity, which is in turn equal to the velocity of the fish divided by the radius of the curve. Velocity was determined by differentiating the distance–time film data with respect to time, using the five-point moving regression method (Lanczos, 1956).

Results

Film analyses of escapes reveal that both species employ the three kinematic stages described by Weihs (1973): preparatory, propulsive and variable. C and S patterns similar to those described by Webb (1976) are also observed, although the mechanics of *E. lucius* suggests two forms of S-shaped fast starts.

Figs 3–7, which have been corrected for tangential acceleration, indicate that there is a functional relationship between the mechanics of the escapes, revealed by the accelerometer, and the kinematics of these patterns, shown by film. These figures show acceleration, velocity and distance travelled (after correcting for tangential acceleration) over the same period. It is assumed that the fast-start terminates when the fish reaches its maximum velocity. Comparisons of escape times with those from previous studies which evaluate performance to the end of stage two (e.g. Webb, 1978*b*), indicate that this is valid. Insets show traces from simultaneous film records of the same events. Although these traces are to scale, they have been realigned on the grid and, as such, they represent the orientation of the fish's body with reference to its original position, not the actual distance travelled.

Trout fast-starts can be categorized into two different mechanical types. During type I fast-starts (Fig. 3) the fish bends into an S, then a C shape (numbers 1 and 3 on Fig. 3, respectively) and turns considerably more than 90° from its original orientation. Maximum acceleration occurs when the head is oriented towards the direction of escape. The acceleration plot for this behaviour is unimodal, rising to one significant peak, then declining. Fig. 4 shows a *S. gairdneri* escape response

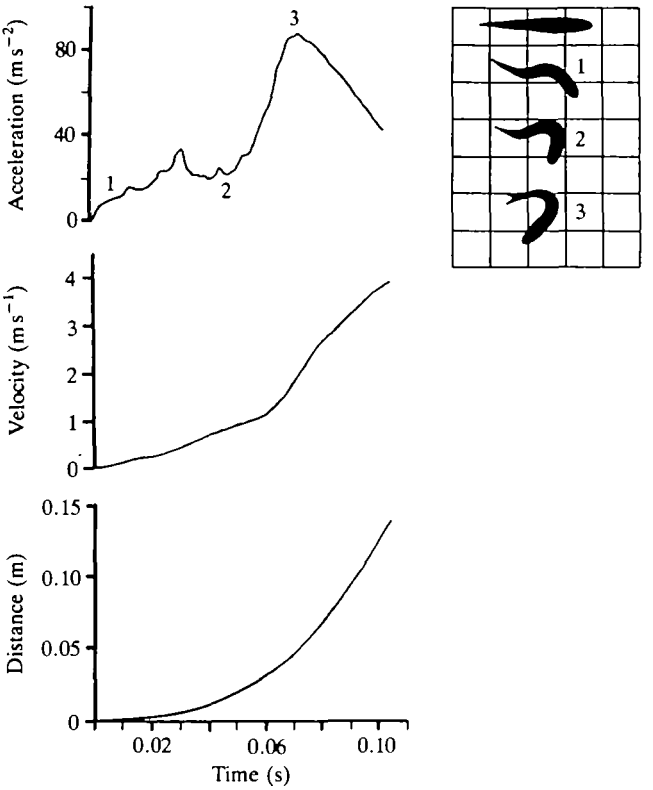

Fig. 3. Mechanical and kinematic data for the type I fast-start of *Salmo gairdneri* (mass=0.488 kg, fork-length=0.370 m), corrected for tangential acceleration, showing acceleration, velocity and distance travelled *versus* time. Numbers on the tracings correspond to those on the acceleration plot. The scale for the grid is 10 cm.

characteristic of a type II fast-start. Note that both acceleration and velocity plots are bimodal. Kinematically, the fish again bends into an S shape (2), but then turns its head back in the original direction of orientation (4). As its body forms a C shape (3), the fish reaches maximal deceleration. Type II escapes involve a turn of about 90° and reach maximum acceleration during the preparatory stage. Relative to the type I escape, a greater distance is covered in the first half of the event, though the total distance travelled is about the same (Table 2).

Fig. 5 shows the unimodal acceleration plot typical of a type I fast-start for *E. lucius*. There are similarities with *S. gairdneri* type I escapes, other than this unimodal shape. For example, *E. lucius* also bends into an S (2), then a C shape (4). Again, the maximum acceleration is recorded when the head is oriented towards its final destination which, as with *S. gairdneri*, is much greater than 90° from its original orientation. The main difference between the two is the magnitude of the performance. The higher acceleration exhibited by *E. lucius* results in a higher final velocity, moving the fish a greater distance in less time.

The type II fast-start of *E. lucius* (Fig. 6) is also similar to that of *S. gairdneri*.

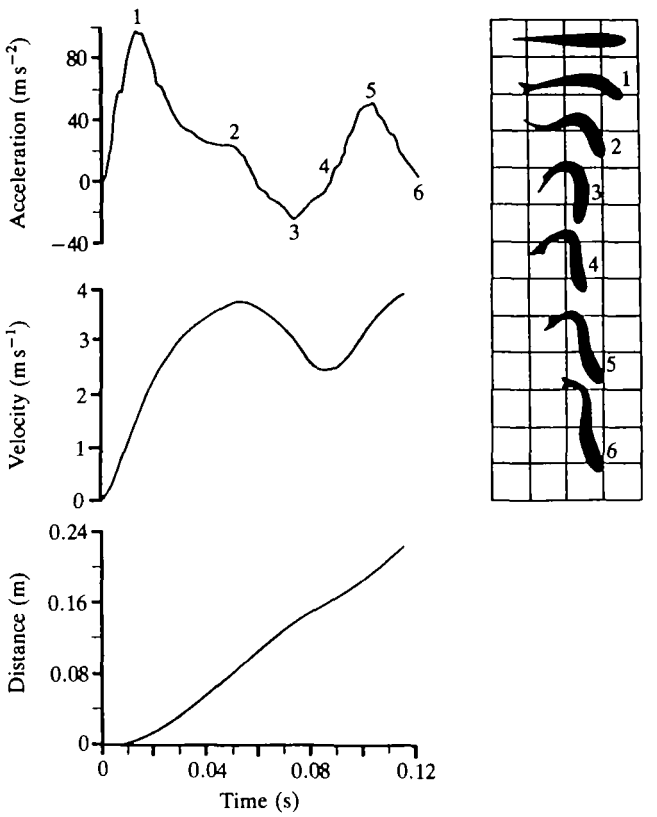

Fig. 4. Mechanical and kinematic data for the type II fast-start of *Salmo gairdneri* (mass=0.488 kg, fork-length=0.370 m).

The bimodal shapes of the acceleration and velocity plots are similar, though the point of maximum acceleration is, consistently, at the peak of the second mode rather than the first, as is the case for *S. gairdneri*. This, and the earlier decelerative phase, make the peak velocity at the first mode lower. In type II starts, *E. lucius*, unlike *S. gairdneri*, never actually bends into a C shape; at maximum deceleration (2) a small degree of reverse curvature is seen at the tail. As with *S. gairdneri*, the final orientation is about 90° from the original one.

Type III fast-starts (Fig. 7) have characteristic trimodal acceleration and velocity plots and are observed during escapes of *E. lucius*. In Fig. 7, the fish almost stops before the third increase in acceleration. Arguably, the objective of this type of fast-start is to maintain directional stability and orient in the same direction as originally aligned. From a still position to orientation (2), the acceleration and kinematics are similar to a type II escape. After this point, a second, reverse S shape is produced by the body which changes course back to the original orientation.

Fifty-five escapes were analyzed; 30 by *S. gairdneri* and 25 by *E. lucius*. The mechanical types described here are representative of each species because all

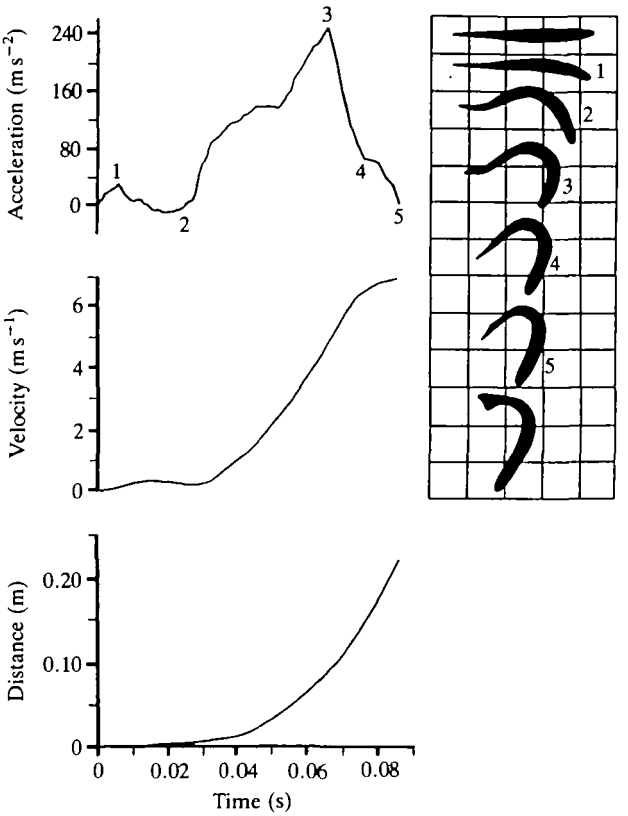

Fig. 5. Mechanical and kinematic data for the type I fast-start of *Esox lucius* (mass=0.377 kg, fork-length=0.376 m).

individuals exhibited the behaviour characteristic of its species and no other behaviour was observed. *S. gairdneri* employed type I escapes 60 % and type II 40 % of the time. Since C and S starts are kinematically similar to type I and II escapes, respectively, these results can be compared to, and are in agreement with, values reported by Webb (1976) for *S. gairdneri* of this size. *E. lucius* exhibited type II escapes 44 % of the time, the remaining fast-starts being divided evenly between type I and III (28 % each).

The magnitude of the tangential acceleration is presented as percentage changes to the accelerometer data in Table 1. The effect on the performance records from the trout is significant; reductions in all performance parameters, apart from maximum acceleration, range from about 20 to 30 %. Pike performance records are affected to a lesser degree, amounting to reductions of the order of 5–10 %. It is of interest that the mean maximum acceleration of pike, as measured by the accelerometer, actually underestimates the true value by 6.4 %. This is due to a tendency for the fish to reach maximum acceleration near the end of the curved portion of the escape trajectory. At this point the rate of change of angular velocity, and therefore tangential acceleration, is negative. The effect of tangential

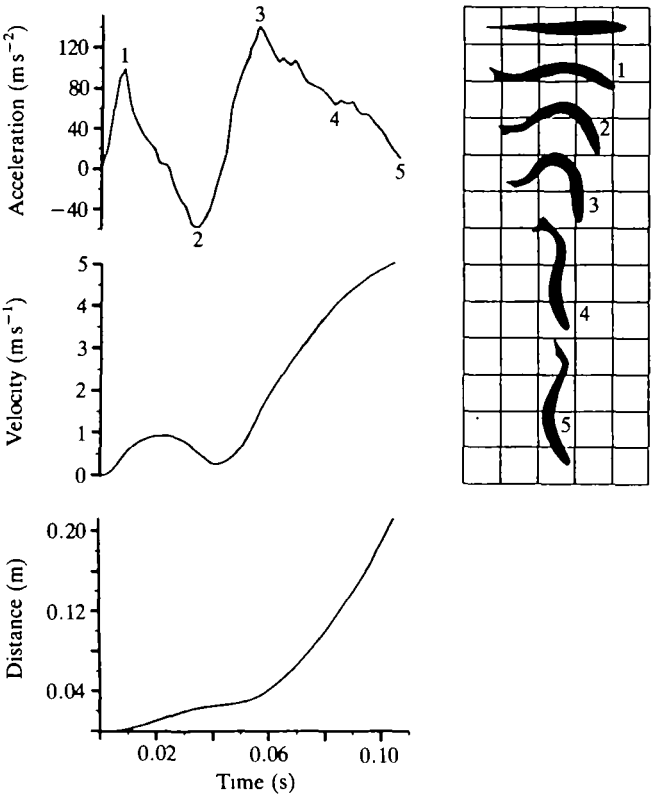

Fig. 6. Mechanical and kinematic data for the type II fast-start of *Esox lucius* (mass=0.372 kg, fork-length=0.363 m).

acceleration on each mechanical fast-start type is also presented in Table 1. It would appear that this factor is of greatest influence during type I fast-starts, because the angular velocities are higher.

Escape performance, measured here with subcutaneously implanted accelerometers, is presented in Table 2. Performance parameters are grouped into mechanical types, and are also presented as totals, combining types, for both *S. gairdneri* and *E. lucius*. The duration of the escapes ranges from 0.085 s for *E. lucius* type I to 0.134 s for *S. gairdneri* type I fast-starts. Distance travelled is greatest for *E. lucius* type III (0.223 m) and least for *S. gairdneri* type I (0.141 m) escapes. The remaining ranges of performance are all least for *S. gairdneri* type I and greatest for *E. lucius* type I behaviour. Mean velocities range from 1.16 to 2.27 m s^{-1}; mean maximum velocities are 2.79 and 4.70 m s^{-1}. Mean acceleration rates from 21.4 to 54.7 m s^{-2} were observed; mean maximum accelerations range from 56.6 to 157.8 m s^{-2}.

Statistical analyses (Table 3) involved first employing the Student's *t*-test to identify differences in performance between species, when all escapes are considered. This indicated significant differences for all performance parameters.

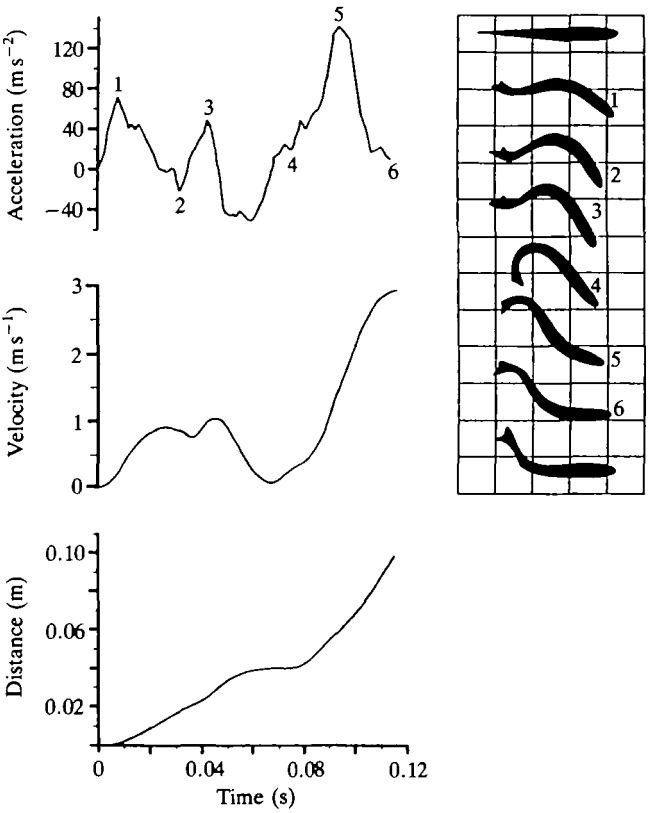

Fig. 7. Mechanical and kinematic data for the type III fast-start of *Esox lucius* (mass=0.322 kg, fork-length=0.356 m).

The data sets were then considered according to mechanical type, for both species. One-way analysis of variance again showed strong significant differences between means for all parameters. Finally Tukey's test was used to indicate where robust differences between means were to be found, considering all possible comparisons.

Table 3 shows that there is no significant difference between the type I and II escapes exhibited by *S. gairdneri*. From Figs 3 and 4, it is evident that the maximum rate of acceleration is reached more quickly in the type II fast-start. From Table 3 it is also evident that no significant differences exist in comparisons of *E. lucius* type II and III fast-starts, nor is there any difference for within-species comparisons of distance or mean maximum velocity. When *E. lucius* type I fast-starts are compared to types II and III, significant differences in performance are identified, particularly with respect to mean and maximum acceleration. In all such comparisons it is the type I behaviour that exhibits the highest performance.

Comparisons of *E. lucius* and *S. gairdneri* escape performance reveal an array of significant differences, particularly where *S. gairdneri* and *E. lucius* type I escapes are compared. In contrast, when compared to *E. lucius* type III escapes, neither of

Table 1. *Mean effect of tangential acceleration on performance data, expressed as percentage changes relative to accelerometer values*

	N	Distance	Mean velocity	Maximum mean velocity	Mean acceleration rate	Mean maximum acceleration
Salmo gairdneri						
Type I	9	−32.6	−34.1	−24.1	−22.3	−6.6
		(±2.1)	(±3.8)	(±3.4)	(±3.0)	(±2.5)
Type II	4	−28.4	−28.6	−18.8	−17.6	−8.8
		(±3.6)	(±3.7)	(±3.8)	(±3.8)	(±3.6)
Total	13	−31.1	−32.4	−22.5	−20.8	−7.3
		(±2.0)	(±3.2)	(±3.2)	(±2.8)	(±2.0)
Esox lucius						
Type I	3	−18.8	−6.8	−9.2	−10.9	10.3
		(±2.6)	(±5.6)	(±4.7)	(±4.4)	(±4.6)
Type II	6	−11.1	−8.5	−3.8	−3.7	4.0
		(±2.9)	(±2.8)	(±2.4)	(±2.4)	(±4.2)
Type III	3	−10.9	−10.5	−9.0	−11.3	7.1
		(±2.8)	(±2.8)	(±2.6)	(±3.0)	(±3.2)
Total	12	−12.5	−8.5	−6.5	−7.4	6.4
		(±2.6)	(±2.7)	(±2.0)	(±2.2)	(±2.8)

Combined data, disregarding mechanical types, for each species are presented as totals.
Errors are given in brackets as ±2 S.E.
Data include samples from all eight trout and four pike.

the *S. gairdneri* behaviour patterns (types I and II) was found to have significantly different mean or maximum acceleration, maximum velocity or duration. When the type II behaviour patterns for each species are compared, similar levels of performances are exhibited, except with reference to mean velocity and maximum acceleration. Where differences are identified, Table 2 indicates that *E. lucius* displays the higher performance.

Discussion

Sources of error

Criticism of the use of accelerometry centres around three major points; the introduction of rotational accelerations due to the curvilinear trajectory, the possibility that transient motion may occur between the body of the fish and the accelerometer, and consideration of the orientation of the instrument with respect to the centre of mass.

Point-by-point analysis of film shows that the trajectory along which the centre of mass travels during a fast-start is not linear, but forms a series of alternating, left- and/or right-hand curves. In fact, any point along the centre-line of the fish will follow these curves, though amplitudes increase with distance from the centre of mass. Since the accelerometer used in this study is firmly implanted parallel to

Table 2. *Results of escape performance for* Salmo gairdneri *and* Esox lucius *determined by accelerometry*

	Total time (s)	Distance (m)	Mean velocity (ms^{-1})	Mean maximum velocity (ms^{-1})	Mean acceleration rate (ms^{-2})	Mean maximum acceleration (ms^{-2})	*N*
Salmo gairdneri							
Type I	0.134 (±0.019)	0.141 (±0.020)	1.16 (±0.19)	2.79 (±0.35)	21.4 (±4.0)	56.6 (±10.1)	18
Type II	0.110 (±0.015)	0.142 (±0.043)	1.29 (±0.27)	2.74 (±0.63)	24.1 (±3.6)	64.7 (±14.3)	12
Total	0.125 (±0.014)	0.141 (±0.020)	1.21 (±0.15)	2.77 (±0.31)	22.4 (±2.8)	59.7 (±8.3)	30
Esox lucius							
Type I	0.085 (±0.005)	0.194 (±0.044)	2.27 (±0.28)	4.70 (±0.52)	54.7 (±7.0)	157.8 (±37.3)	7
Type II	0.110 (±0.013)	0.192 (±0.032)	1.76 (±0.18)	3.69 (±0.46)	33.2 (±5.0)	107.9 (±16.4)	11
Type III	0.132 (±0.013)	0.223 (±0.027)	1.72 (±0.31)	3.61 (±0.68)	25.1 (±6.6)	91.4 (±22.8)	7
Total	0.108 (±0.010)	0.201 (±0.020)	1.90 (±0.17)	3.97 (±0.36)	37.6 (±6.1)	120.2 (±20.0)	25

Errors are given in brackets as ±2 S.E.
Totals combine data, regardless of mechanical type, for each species.
Eight trout and four pike were used.

the centre-line of the fish, it will also follow a curved trajectory. The accelerometers employed here are sensitive only along the long axis of the instrument, so they record only in the forward (and rearward) direction, at any time. They will, however, detect rotational accelerations tangential to the curved trajectory. Tangential accelerations can be calculated, and accelerometer values corrected, assuming film data are available. Table 1 shows that this correction is not consistent for all performance parameters and that it varies between species. The relative changes in performance values (except maximum acceleration) for *S. gairdneri* are about three times those of *E. lucius*. This is primarily due to two factors; *S. gairdneri* escapes have curvatures of smaller radii and longer duration and, though the absolute values for tangential acceleration are similar, they represent proportionally lower values in *E. lucius*, owing to the higher levels of performance.

Because of tangential accelerations, the use of accelerometry requires simultaneous film data when trajectories are curved. However, for stereotypic events this component of acceleration, and its effect on predicted velocities and distances, can be determined initially, then factored into subsequent events measuring performance by accelerometry alone. Table 2 also shows that studies evaluating

Table 3. *Descriptive statistics for comparison of escape performance both within and between species*

Comparison	Time (s)	Distance (m)	Mean velocity ($m s^{-1}$)	Mean maximum velocity ($m s^{-1}$)	Mean acceleration rate ($m s^{-2}$)	Mean maximum acceleration ($m s^{-2}$)
Salmo gairdneri						
Type I *vs* II	NS	NS	NS	NS	NS	NS
Esox lucius						
Type I *vs* II	NS	NS	$P<0.05$	NS	$P<0.001$	$P<0.01$
Type I *vs* III	$P<0.025$	NS	NS	NS	$P<0.001$	$P<0.005$
Type II *vs* III	NS	NS	NS	NS	NS	NS
Salmo (S) vs Esox (E)						
*S*I *vs E*I	$P<0.001$	NS	$P<0.001$	$P<0.001$	$P<0.001$	$P<0.001$
*S*I *vs E*II	NS	NS	$P<0.001$	$P<0.05$	$P<0.005$	$P<0.001$
*S*I *vs E*III	NS	$P<0.025$	$P<0.025$	NS	NS	NS
*S*II *vs E*I	NS	NS	$P<0.001$	$P<0.001$	$P<0.001$	$P<0.001$
*S*II *vs E*II	NS	NS	$P<0.05$	NS	NS	$P<0.05$
*S*II *vs E*III	NS	$P<0.05$	NS	NS	NS	NS
Total*	$P<0.05$	$P<0.001$	$P<0.001$	$P<0.001$	$P<0.001$	$P<0.001$

Probabilities are indicated; NS denotes comparisons that are not significantly different. Where a significant difference is indicated, reference to Table 2 will reveal which is the larger.

Tukey's test is used for all comparisons except where combined data, regardless of mechanical type, are compared using the two-sample Student's *t*-test (*).

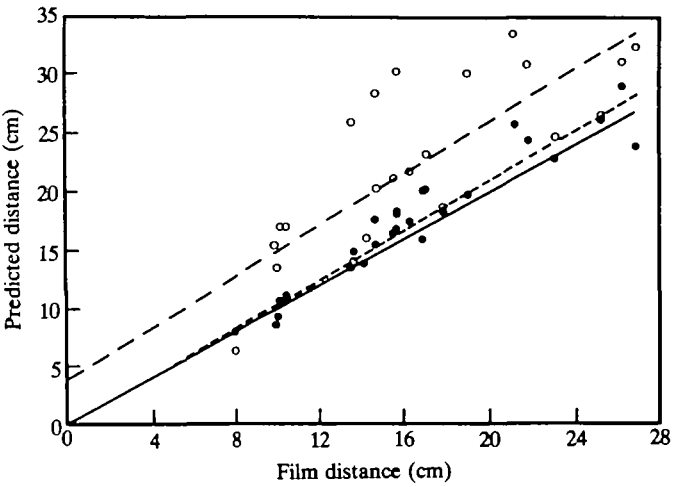

Fig. 8. Predicted escape displacements compared to film data. The solid line represents film data *vs* themselves, for comparison with accelerometer predictions of distance (open circles) and corrected predictions (closed circles) once tangential accelerations have been considered. Regression lines have r^2 values of 0.68 for accelerometer data (long-dashed line) and 0.94 for corrected data (short-dashed line).

only maximum accelerations would be much less influenced by tangential accelerations.

The orientation of the accelerometer with respect to the centre of mass is important because misalignment would cause the instrument to detect a component of centripetal acceleration, which is directed perpendicular to the tangent of the curved trajectory (and is not, therefore, normally realized by the directionally biased accelerometer). A worst-case scenario, where the accelerometer was oriented 10° from the tangent to the curve, was investigated. Several escapes were re-evaluated in this manner, considering all components of acceleration. Comparisons with accelerations assuming perfect alignment showed that the net effect was maximally less than 5 %.

Another important consideration when employing accelerometry is that tissue flexibility could introduce transient motions between the musculature of the fish and the accelerometer. With respect to this problem, and that of accelerometer orientation, it is worth reiterating the importance of ensuring proper implantation by following the procedure described earlier. To estimate the effect of both transient motion and orientation on accelerometer data, values for displacement, as predicted by film and accelerometry, were compared (Fig. 8). Had these two factors produced significant effects on acceleration this would be propagated through the integrations giving velocity and distance data. Fig. 8 shows that once tangential acceleration is considered, the difference between film and accelerometer estimations of displacement is small. Incidentally, this comparison would also account for any other sources of error in the accelerometer data.

Damping and linearity are not significant sources of error with the acceler-

ometers used here. The high-frequency response (125 kHz) precludes the possibility of phase shifts. The linearity of the response is reported to be 1%, maximally, at 1000 g. Since the maximum accelerations recorded here are of the order of 25 g, the error arising from poor linearity is likely to be extremely small. Another potential problem is the calibration of the accelerometers. The accelerometers used here are calibrated using a back-to-back comparison technique against a reference standard. They were also calibrated in the laboratory to determine how output voltage translates to actual accelerations.

Comparison with previous studies

Results of previous studies are presented, in chronological order, in Table 4. Since all performance parameters were rarely reported, some of the data in Table 4 had to be calculated from that given, or from given formulae. Research evaluating only displacements is not included because this study focuses on other aspects of performance, particularly acceleration. Data from Eaton *et al.* (1977) are also omitted, because their performance was measured with respect to the rostral tip of the nose. Webb (1978*b*) explains why such comparisons are unjustified. Therefore Table 4 is not comprehensive, but does reflect the bulk of previous performance data of the sort measured here.

Previous reports of mean maximum acceleration during escapes are as high as 50 m s^{-2} for pike *E. lucius* (Weihs, 1973). Webb (1978*b*) found values of 40 m s^{-2} for teleosts, with 95% confidence limits of ±25% of the mean, though an individual smallmouth bass was reported to have accelerated at 110 m s^{-2} (Webb, 1983). Mean acceleration rates for rainbow trout *S. gairdneri*, chain pickerel *Esox niger* and tiger musky *Esox* sp. are, maximally, about 20 m s^{-2} (Weihs, 1973; Rand and Lauder, 1981; Webb, 1986, respectively). Maximum velocities range up to 2.85 m s^{-1} for *S. gairdneri*, with mean velocities for the same species of 1.63 m s^{-1} (Webb, 1976). Fast-start durations range from about 0.056 s for *Etheostoma caeruleum* (Webb, 1978*b*) to 0.323 s for larvae of the northern anchovy *Engraulis mordax* (Webb and Corolla, 1981).

Comparisons of results reported here employing accelerometry (Table 2) with film-based studies (Table 4) demonstrate that, while most performance parameters for *S. gairdneri* fall near the high range of previous results (with the exception of maximum acceleration), the values for *E. lucius* greatly exceed previously reported data for any species. The reason for the large disparity of mean maximum accelerations for both species is probably the large degree of error inherent in evaluating accelerations from double-differentiated, film-generated distance–time data. Harper and Blake (1989) show that when determined from film, maximum accelerations incorporate errors of 35–100% of reported values for the range of sampling rates in Table 4. Only one previous study (Webb, 1978*b*) assesses a member of the genus *Esox* in a comprehensive manner. It is possible that the fish used in that study were performing sub-maximally. Table 4 indicates that high levels of escape performance are exhibited by *E. lucius*. It is therefore

Table 4. *Chronological review of comprehensive fast-start performance data reported in the literature*

	Mean maximum acceler-ation (ms^{-2})	Mean acceler-ation rate (ms^{-2})	Mean maximum velocity (ms^{-1})	Mean velocity (ms^{-1})	Distance (m)	Time (s)	Species	Common name	Length (m)	Method	Rate (Hz)
Weihs (1973)	40.0	–	–	–	–	–	*Salmo trutta*	Trout	–	Film	–
	50.0	–	–	–	–	–	*Esox*	Pike	–	Film	–
	25.5	20.6	–	0.57†	0.113‡	0.200‡	*Salmo gairdneri*	Rainbow trout	0.330	Film	40
Webb (1975)	42.1	12.1	1.21	0.72†	0.056	0.078	*Salmo gairdneri*	Rainbow trout	0.143	Film	64
	15.7	8.1	0.67	0.36†	0.029	0.079	*Lepomis cyanellus*	Green sunfish	0.080	Film	64
	95.0	–	–	–	–	–	*Salmo gairdneri*	Rainbow trout	–*	Film	64
Dubois *et al.* (1976)	23.5	–	2.80	–	–	0.210	*Pomotamus saltatrix*	Bluefish	0.630*	Accelerometer	
Webb (1976)	40.6	17.6	2.85	1.63†	0.163	0.100	*Salmo gairdneri*	Rainbow trout	0.387	Film	64
Webb (1977)	26.6	8.6	1.44	0.70†	0.076	0.109	*Salmo gairdneri*	Rainbow trout	0.174	Film	250
Webb (1978*a*)	41.0	–	1.71	1.13†	0.113	0.100	*Salmo gairdneri*	Rainbow trout	0.136	Film	250
Webb (1978*b*)	39.5	10.4	1.56	0.73	0.084‡	0.115‡	*Esox* sp.	Tiger musky	0.217	Film	250
	32.6	10.6	1.58	0.75	0.085‡	0.114‡	*Salmo gairdneri*	Rainbow trout	0.195	Film	250
	23.9	9.3	1.15	0.50	0.051‡	0.103‡	*Perca flavescens*	Yellow perch	0.155	Film	250
	28.8	12.3	1.30	0.67	0.059‡	0.088‡	*Lepomis macrochirus*	Bluegill	0.153	Film	250
	28.7	11.0	1.14	0.49	0.038‡	0.078‡	*Notropis cornutus*	Common shiner	0.107	Film	250
	22.7	6.1	0.77	0.43	0.035‡	0.081‡	*Cottus cognatus*	Slimy sculpin	0.082	Film	250
	32.3	10.3	0.89	0.43	0.024‡	0.056‡	*Etheostoma caeruleum*	Rainbow darter	0.062	Film	250
Rand and Lauder (1981)	–	21.1†	2.47†	1.08†	0.100†	0.092	*Esox niger*	Chain pickerel	0.273	Film	200
Webb and Corolla (1981)	–	–	0.38†	0.21†	0.068†	0.323	*Engraulis mordax*	Northern anchovy	0.013**	Film	250
Webb (1982)	–	–	–	1.01†	0.147§	0.146	*Salmo gairdneri*	Rainbow trout	0.298	Film	240
Webb (1983)	80.0	–	2.50	–	–	–	*Salmo gairdneri*	Rainbow trout	0.257*	Film	60
	110.0	–	2.50	–	–	–	*Micropterus dolomieu*	Smallmouth bass	0.236*	Film	60
Webb (1986)	–	19.0‡	1.36	–	–	–	*Esox* sp.	Tiger musky[1]	0.065	Film	60
	–	16.0‡	–	–	–	–	*Esox* sp.	Tiger musky[2]	0.065	Film	60
	–	15.0‡	0.96	–	–	–	*Micropterus salmoides*	Largemouth bass	0.051	Film	60
	–	14.5‡	1.01	–	–	–	*Lepomis macrochirus*	Bluegill	0.064	Film	60
	–	11.5‡	0.81	–	–	–	*Pimephales promelas*	Fathead minnow	0.058	Film	60

*Single event; **larval fish; †calculated from data; ‡read from figures; §calculated from formulae; [1] S-type start; [2] C-type start.
Studies reporting displacements only, or those evaluating performance with respect to points other than the centre of mass, are omitted.

not surprising to find higher levels of performance in this species, considering the advanced methodology.

Maximum performance

Except for escape duration (given accurately by film), the performance values reported in Table 2 are the highest yet reported for *E. lucius*. These are mean values, however, averaged for a number of specimens, each executing a number of fast-starts. This is necessary when making the statistical comparisons summarized in Table 3. It is also important when using this information in ecological models, such as those that predict feeding energetics or daily energy budgets.

The limits of performance (single, maximum performance, fast-starts) are also of interest because such information is useful in assessing the energetic cost of unsteady swimming, optimal behaviour during predator–prey interactions, and feeding efficiency of ambush predators, to name but a few applications. Also, since fish are stimulated artificially, under laboratory conditions, it is likely that they do not always react maximally, as they would to a predator, and may habituate to the stimulus. Reporting maximum values (Table 3), therefore, is important because it reveals the fish's capability under extreme conditions. Table 2 shows that *E. lucius* employs escape behaviour patterns other than those that would maximize performance. This implies that the fish are, at times, performing sub-maximally under experimental conditions.

Table 5 lists the maximum levels of performance for both species, for each type of escape. Performance values are much higher than any previously reported for *S. gairdneri* and *E. lucius*. In fact, the absolute values reported here for the *E. lucius* type I escape are the highest reported for any fish. Webb (1975, 1978*b*, respectively) does report single maximum accelerations of 95 m s^{-2} for *S. gairdneri* and 110 m s^{-2} for *Micropterus dolomieu*, but this was derived from film recorded at 64 and 60 Hz, respectively, which Harper and Blake (1989) show to involve an error of about 100 %.

Table 5. *Maximum levels of performance for all escape types exhibited by* Salmo gairdneri *(mass=0.488 kg, fork-length=0.370 m) and* Esox lucius *(mass=0.377 kg, fork-length=0.376 m)*

	Distance (m)	Mean maximum velocity (m s^{-1})	Maximum final velocity (m s^{-1})	Maximum mean acceleration (m s^{-2})	Maximum acceleration rate (m s^{-2})
Salmo gairdneri					
Type I	0.149	1.87	4.19	32.6	95.7
Type II	0.223	1.93	3.94	32.0	97.8
Esox lucius					
Type I	0.213	2.50	7.06	80.3	244.9
Type II	0.289	2.26	4.70	47.4	141.2
Type III	0.227	2.14	4.50	35.5	130.5

Comparison between species

This is the first study to demonstrate conclusive differences in mean and maximum accelerations for fish of different body forms. Webb (1978*b*) concluded that these performance parameters were independent of body form. In a later study relating escape behaviour to body form for teleost prey, Webb (1986) claims that tiger musky *Esox* sp. had the highest mean acceleration rates, followed by bluegill *Lepomis macrochirus*, largemouth bass *Micropterus salmoides* and fathead minnow *Pimephales promelas*. However, the study used 60 Hz video film to determine acceleration which, as stated previously, is subject to large error. In the same study, Webb derives an acceleration coefficient – a dimensionless factor relating the product of motor (muscle) and propellor (body and tail) thrust to the mass accelerated. This indicates that fish forms such as *E. lucius* have the highest acceleration coefficients, while those with morphologies like *S. gairdneri* have lower coefficients.

Fish morphologies have evolved, in part, as a response to two functionally different hydrodynamic requirements: one specialized for long-distance swimming, the other for rapid lunges (Weihs and Webb, 1983). Results here indicate that *E. lucius* is capable of much higher escape (lunging) performance than is *S. gairdneri* of similar size. This supports previous suggestions (Weihs, 1973; Lighthill, 1975; Weihs and Webb, 1983; Webb, 1986) that the body form of *E. lucius* is well adapted to this type of behaviour. The body form of *S. gairdneri* is considered to be that of a generalist, displaying some characteristics that enhance steady swimming and some that benefit fast-starts (Webb, 1978*b*).

Fast-start types

The integration of mechanics and kinematics (Figs 3–7) affords more detailed insight into fish fast-starts. In addition to simple kinematic categorizations, such as C and S patterns (Webb, 1976), it is clear that a mechanical basis underlies the kinematic observations. Accelerometer plots reveal that at least three different types of fast-starts exist: uni-, bi- and trimodal. Dubois *et al.* (1976; Fig. 4) also provide acceleration–time plots which indicate type I and type II escapes in a bluefish *Pomatomus saltatrix*. However, because the elapsed time of this event is an order of magnitude longer than the events described here, and because the correlation with kinematics is not as obvious, a direct comparison is not possible. However, a recent film study on the fast-start performance of the angelfish *Pterophyllum* sp. has also shown all three types of fast-starts described here (P. Domenici, personal communication).

Levels of performance of northern pike *Esox lucius* and rainbow trout *S. gairdneri* are shown to be both significantly different from each other and, for *E. lucius*, higher than previously reported from studies employing film analysis. In this light, it can be concluded that the fast-start performance of fish is dependent on body form. Furthermore, analysis of escape performance, through accelerometry, demonstrates a mechanical basis on which to catagorize this behaviour.

We would like to thank the Natural Science and Engineering Research Council of Canada for financial support. We would also like to thank Dr R. McNeil Alexander, Dr T. Daniel, Dr B. Ahlborn, and two anonymous referees for their valuable comments on an earlier draft of this paper.

References

DuBois, A. B., Cavagna, G. A. and Fox, R. S. (1976). Locomotion of bluefish. *J. exp. Zool.* **195**, 223–226.

Eaton, R. C., Bombardieri, R. A. and Meyer, D. L. (1977). The Mauthner-initiated startle response in teleost fish. *J. exp. Biol.* **66**, 65–81.

Eaton, R. C., DiDomineco, R. and Nissanov, J. (1988). Flexible body dynamics of the goldfish C-start: implications for reticulospinal command mechanisms. *J. Neurosci.* **8**, 2758–2768.

Eaton, R. C., Nissanov, J. and Wieland, C. M. (1984). Differential activation of Mauthner and non-Mauthner startle circuits in the zebrafish: implications for functional substitution. *J. comp. Physiol.* A **155**, 813–820.

Fierstine, H. L. and Walters, V. (1968). Studies of locomotion and anatomy of scombroid fishes. *Mem. Southern Calif. Acad. Sci.* **6**, 1–31.

Gero, D. R. (1952). The hydrodynamic aspects of fish propulsion. *Am. Mus. Novit.* **1601**, 1–32.

Gray, J. (1953). The locomotion of fishes. In *Essays in Marine Biology*. Elmhirst Memorial Lectures (ed. S. M. Marshall and P. Orr), pp. 1–16. Edinburgh: Oliver and Boyd.

Harper, D. G. and Blake, R. W. (1988). Energetics of piscivorous predator–prey interactions. *J. theor. Biol.* **134**, 59–76.

Harper, D. G. and Blake, R. W. (1989). A critical analysis of the use of high-speed film to determine maximum accelerations of fish. *J. exp. Biol.* **142**, 465–471.

Hertel, H. (1966). *Structure, Form and Movement*. New York: Reinhold.

Lanczos, C. (1956). *Applied Analysis*. Englewood Cliffs: Prentice Hall.

Lauder, G. V. (1982). Structure and function in the tail of the pumpkinseed sunfish (*Lepomis gibbosus*). *J. Zool., Lond.* **197**, 483–495.

Lighthill, M. J. (1975). *Mathematical Biofluiddynamics*. Philadelphia: Society for Industrial and Applied Mathematics.

Meriam, J. L. (1975). *Dynamics: Second Edition – SI Version*. Toronto: John Wiley & Sons, Inc.

Rand, D. M. and Lauder, G. V. (1981). Prey capture in the chain pickerel, *Esox niger*: correlations between feeding and locomotor behaviour. *Can. J. Zool.* **59**, 1072–1078.

Richardson, S. C. (1985). Effects of sampling on blood parameters in the rainbow trout. *J. Fish Biol.* **26**, 725–732.

Tilley, D. E. and Thumm, W. (1974). *Physics for College Students with Applications to the Life Sciences*. Menllo Park, CA: Cummings Publishing Company.

Webb, P. W. (1975). Acceleration performance of rainbow trout *S. gairdneri* and green sunfish *Lepomis cyanellus*. *J. exp. Biol.* **63**, 451–465.

Webb, P. W. (1976). The effect of size on the fast-start performance of rainbow trout *S. gairdneri*, and a consideration of piscivorous predator–prey interactions. *J. exp. Biol.* **65**, 157–177.

Webb, P. W. (1977). Effects of median-fin amputation on fast-start performance of rainbow trout (*S. gairdneri gairdneri*). *J. exp. Biol.* **68**, 123–135.

Webb, P. W. (1978*a*). Temperature effects on acceleration of rainbow trout S. *gairdneri*. *J. Fish. Res. Bd Can.* **35**, 1417–1422.

Webb, P. W. (1978*b*). Fast-start performance and body form in seven species of teleost fish. *J. exp. Biol.* **74**, 211–226.

Webb, P. W. (1983). Speed, acceleration, and manoeuvrability of two teleost fishes. *J. exp. Biol.* **102**, 115–122.

Webb, P. W. (1984). Chase response latencies of some teleostean piscivores. *Comp. Biochem. Physiol.* A **97**, 45–48.

Webb, P. W. (1986). Effect of body form and response threshold on the vulnerability of four species of teleost prey attacked by largemouth bass (*Micropterus salmoides*). *Can. J. Fish. aquat. Sci.* **43**, 763–771.

WEBB, P. W. AND COROLLA, R. T. (1981). Burst swimming performance of northern anchovy, *Engraulis mordax*, larvae. *Fish. Bull.* **79**, 143–150.
WEBB, P. W. AND SKADSEN, J. M. (1980). Strike tactics of *Esox*. *Can. J. Zool.* **58**, 1462–1469.
WEIHS, D. (1973). The mechanism of rapid starting of slender fish. *Biorheology* **10**, 343–350.
WEIHS, D. AND WEBB, P. W. (1983). Optimization of locomotion. In *Fish Biomechanics* (ed. P. W. Webb and D. Weihs), pp. 339–371. New York: Praeger.